INSTABILITY PROCESSES FOR MAGNONS IN FERROMAGNETIC NANOSTRUCTURES

BY MICHAEL G. COTTAM AND ZAHRA HAGHSHENASFARD

An understanding of the magnetization dynamics, both linear and nonlinear, in ordered magnetic materials such as ferromagnets is of fundamental interest and also has applications for various high-frequency and switching devices in the expanding fields of spintronics and magnonics. Here we describe some nonlinear processes in ultrathin films and nanowires, where the fundamental excitations of the systems, known as spin waves or magnons, are strongly influenced by their spatial confinement in the nanosystem and can be driven into a decay instability by application of a microwave-frequency electromagnetic wave above a high-power threshold level.

INTRODUCTION

A description of the wave-like fluctuations in unbounded ferromagnets (i.e., where boundary effects are negligible) in terms of "spin waves" is well known and given in most solid-state physics and magnetism textbooks [1,2]. When the quantum-mechanical nature of the spin operators is taken into account, the excitations are called "magnons", by analogy with phonons as the quantized lattice vibrations in a solid. It is often helpful to picture magnons schematically as in Fig. 1 in terms of arrays of precessing spin vectors, where there is a small change of phase (related to the wave vector) from any one spin to a neighbouring spin. In this semi-classical viewpoint the precession of a spin vector takes place due to the torque from an effective magnetic field that incorporates all the magnetic interactions with other spins as well as any applied magnetic field. In simple cases (such as at low temperatures compared with the Curie temperature T_C) the angle of precession is small, meaning that the component of the spin vector along the direction of net magnetization remains approximately constant.

SUMMARY

The nonlinear magnetization dynamics in ferromagnetic nanostructures are studied through the parametric instabilities of the interacting magnons in thin films and nanowires under microwave pumping.

The dispersion relation of the magnons, which gives the angular frequency $\omega(\mathbf{k})$ of precession in terms of the wave vector $\mathbf{k}$, depends on the nature of the interactions. These arise mainly from (a) the short-range exchange interactions, which are quantum-mechanical in nature and are due to the overlap of wave functions on neighboring atoms, and (b) the long-range magnetic dipole-dipole interactions as in classical electromagnetism. If a Hamiltonian formalism is employed, the contributions to the energy from these terms [1–3] are, respectively, proportional to $J(r_{12})\mathbf{S}_1\cdot\mathbf{S}_2$ and $\mu_B^2[\mathbf{S}_1\cdot\mathbf{S}_2-3(\mathbf{S}_1\cdot\hat{\mathbf{r}}_{12})(\mathbf{S}_2\cdot\hat{\mathbf{r}}_{12})]/r_{12}^3$, where subscripts 1 and 2 label spin operators at different atomic sites at a distance r_{12} apart connected by unit vector $\hat{\mathbf{r}}_{12}$. The interaction strength J before the exchange term is important typically only between nearest neighbours, whereas the weaker dipolar terms (with μ_B denoting the Bohr magneton) have a more complicated directional dependence and fall off slowly like $1/r_{12}^3$.

A simple calculation of the magnon frequency, applicable for the one-dimensional (1D) system in Fig. 1 with the assumption that only exchange effects occur, is given, for example, in the book by Kittel [1]. This is based on using the torque equation of motion for each spin vector and seeking travelling-wave solutions for the fluctuating components. The final result is that ω increases as the 1D wave vector k increases, being proportional to $SJ(ka)^2$ at small wave vector such that $ka \ll 1$, where a is the distance between spins and S is the spin quantum number.

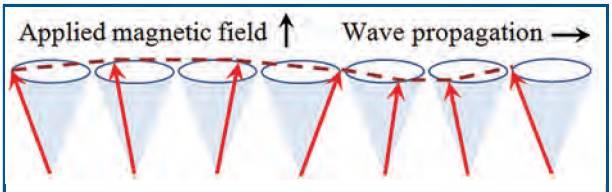

Fig. 1 Schematic illustration of a spin wave (or magnon), taking for simplicity a long line of spin vectors (red arrows), undergoing precession about the direction of net magnetization, defined by the applied magnetic field. One complete wavelength of propagation is depicted, where the dashed line joining the heads of arrows is drawn as a guide to the eye to highlight the wave-like character.

Michael G. Cottam
<cottam@uwo.ca>

and

Zahra Haghshenasfard
<zhaghshe@uwo.ca>

Department of Physics and Astronomy, University of Western Ontario, London, ON N6A 3K7

This result would be modified if effects due to dipolar terms and an applied magnetic field were included [2,3].

A general consequence of the competing interactions is that in reciprocal space, when a Fourier transform is made to a wave-vector representation, the exchange terms dominate at medium and large wave vectors in the Brillouin zone, but the dipolar terms are important at small enough wave vectors. Typically in bulk ferromagnets the dipolar terms need to be included for wave vectors less than about 1/100 of the Brillouin zone boundary value, which is relevant for experimental techniques such as ferromagnetic resonance (FMR) and Brillouin light scattering (BLS) that probe the so-called magnetostatic and dipole-exchange regimes [2,3].

INTERACTING MAGNON GAS

The magnons, when treated in the simplest linear-wave approximation can be shown to behave as bosons, and the number of thermally-excited magnons with energy $\hbar\omega(\mathbf{k})$ is described by the Bose-Einstein distribution function. In reality the magnon states are not exact eigenfunctions of the Hamiltonian, and consequently the magnons constitute a weakly interacting boson gas. In the semiclassical spin-wave picture, the origin of the magnon-magnon interactions is associated with the role of the finite angle of spin precession in changing the longitudinal spin projection. Quantum mechanically the spin operators, which are analogous to the orbital angular momentum operators, do not satisfy the boson commutation relationships, and a mathematical transformations between spin operators and boson operators has to be applied [2,3].

The Hamiltonian for the interacting magnon gas of a ferromagnet, in the notation of second quantization, can be expressed as

$$H = \sum_{\mathbf{k},l} \omega_l(\mathbf{k}) b^+_{\mathbf{k},l} b_{\mathbf{k},l} + H^{(3)} + H^{(4)} + \cdots \qquad (1)$$

in leading order (at temperatures well below T_C), apart from a constant term. Here $b^+_{\mathbf{k},l}$ and $b_{\mathbf{k},l}$ are the creation and annihilation operators, respectively, for a magnon of wave vector $\mathbf{k}$ and branch l. For a bulk (effectively unbounded) material we have only $l = 1$, but this will not generally be so for nanostructures. The first term on the right of Eq. (1) has a form similar to that for the treatment of a simple-harmonic oscillator in quantum mechanics. The next two terms, $H^{(3)}$ and $H^{(4)}$, describe the leading-order three-magnon and four-magnon interaction processes, respectively. The first of these involves operator products like $b^+_{\mathbf{k}',l'} b^+_{\mathbf{k}-\mathbf{k}',l''} b_{\mathbf{k},l}$ and its Hermitian conjugate, which represent magnon splitting (i.e., a magnon is annihilated and two magnons are created) or the corresponding confluence. The last term in Eq. (1) involves products of four boson operators, e.g., two creation and two annihilation operators as for a pair of magnons scattering off one another to produce two other magnons with different wave vectors. It can be shown that the three-magnon processes are due to magnetic dipole-dipole interactions, whereas four-magnon scattering has contributions coming from both the exchange and dipolar interactions [2,3].

MAGNONS IN NANOSTRUCTURES

As mentioned, the magnons for a simple bulk ferromagnet in three dimensions are characterized by a 3D wave vector $\mathbf{k}$ and the branch label l is single-valued. By contrast, in magnetic nanostructures, where one (or more) of the spatial dimensions is of order tens or hundreds of nanometres, the magnons are spatially confined and are required to satisfy boundary conditions at the surfaces or interfaces. In a thin film, for example, the magnons are characterized by a 2D wave vector in the directions of translational symmetry parallel to the surfaces. For the direction perpendicular to the surfaces, the magnons may either take a standing-wave form with a quantized value for the third wave-vector component, or they may be localized with amplitude decaying away from one or both surfaces. Likewise in a nanowire there is a 1D wave vector along the length and standing-mode behaviour or localization in the other two directions.

An example is given in Fig. 2 showing the calculated dispersion relations for the lowest magnon branches in a Permalloy ($Ni_{80}Fe_{20}$) nanowire stripe with rectangular cross section 50 nm by 10 nm and in a longitudinal applied magnetic field of 0.202 T. The frequencies, which were obtained using a microscopic dipole-exchange theory [4] in which magnon interactions are ignored, are plotted versus the 1D wave vector in the small $|\mathbf{k}|$

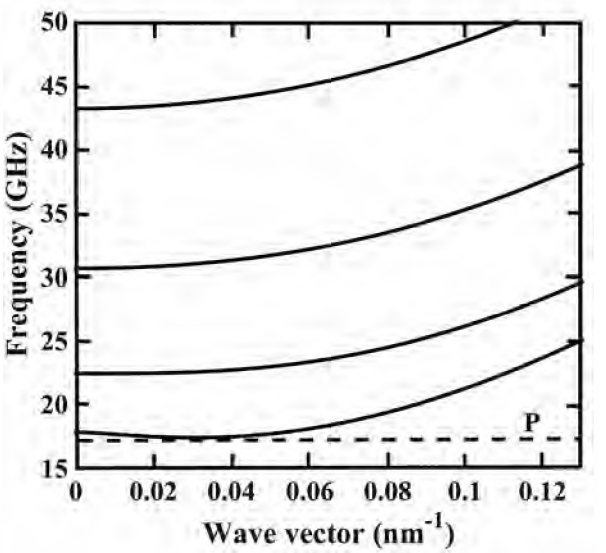

Fig. 2 Dispersion relations, showing frequency versus 1D longitudinal wave vector, calculated for the lowest quantized magnons in a Permalloy nanowire (see text). The horizontal line labeled P is drawn at one half of the pumping frequency considered later.

regime accessible by FMR and BLS measurements. The initial dip for some branches, which is more pronounced for the lowest branch and has been confirmed experimentally, is due to the dipolar interactions competing with the exchange that eventually dominates at larger $|\mathbf{k}|$.

MAGNON INSTABILITIES UNDER MICROWAVE PUMPING

Typically FMR experiments are carried out at relatively low power levels; an oscillating magnetic field at microwave frequency is applied to a ferromagnet in a direction transverse to the magnetization direction. The microwave field can couple linearly to the oscillating magnetic moment of a magnon such that there is a resonant absorption of energy when a match is achieved (e.g., by scanning the static applied field) between the microwave frequency and the precessional frequency of the magnon [1]. Measurement of the FMR linewidth can yield information about the magnon damping (or reciprocal lifetime). This is long established for macroscopically large samples, but for nanostructures such as nanowires the experimental [5] and theoretical [6] studies are quite recent.

For bulk samples it was noticed that, when the signal power was increased in FMR experiments, the absorption strength for the main resonance reached saturation (instead of increasing further) and a subsidiary resonance appeared at higher frequency [7]. Subsequently these nonlinear effects with perpendicular microwave pumping were explained by Suhl [8] in terms of parametric instabilities involving the three- and four-magnon processes, respectively. They are now known as the first-order and second-order Suhl processes, respectively. An analogous instability under parallel microwave pumping was later identified by Schlömann and others [9]. The three types of processes are depicted schematically in Fig. 3; there are several reviews (mainly for macroscopic samples) giving details [2,3,10].

The outcome in all three processes is the production of a pair of magnons with wave vectors $\mathbf{k}$ and $-\mathbf{k}$ of equal magnitude, implying that they have the same frequency. Parallel pumping (Fig. 3a) relies on the fact that the dipolar interactions cause the spin precession to be elliptical rather than circular. Hence the parallel (or longitudinal) components of the spin vectors, which are coupled to the pumping field, fluctuate resulting in the excitation of a magnon pair. The first- and second-order Suhl processes (Figs. 3b and 3c) involve the excitation initially of one (or two) uniform-precession magnons, meaning modes with $\mathbf{k} = 0$, followed by the production of the magnon pair via the $H^{(3)}$ and $H^{(4)}$ interaction terms. From considerations of energy conservation it follows that the angular frequency of each magnon produced in the parallel pumping and first-order Suhl processes is $\frac{1}{2}\omega_p$, whereas in the second-order Suhl process it is ω_p.

In a nanowire, however, the absence of wave-vector conservation in the directions perpendicular to its length gives two

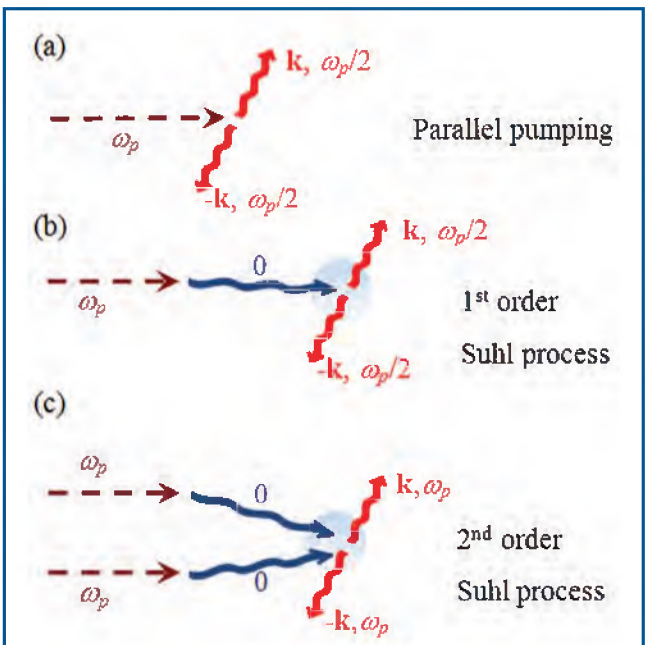

Fig. 3 Schematic representation of the three parametric instability processes under pumping by a microwave field: (a) parallel pumping, (b) first-order Suhl process, and (c) second-order Suhl process. The last two processes occur in perpendicular pumping and involve intermediate uniform-precession (zero wave vector) magnons.

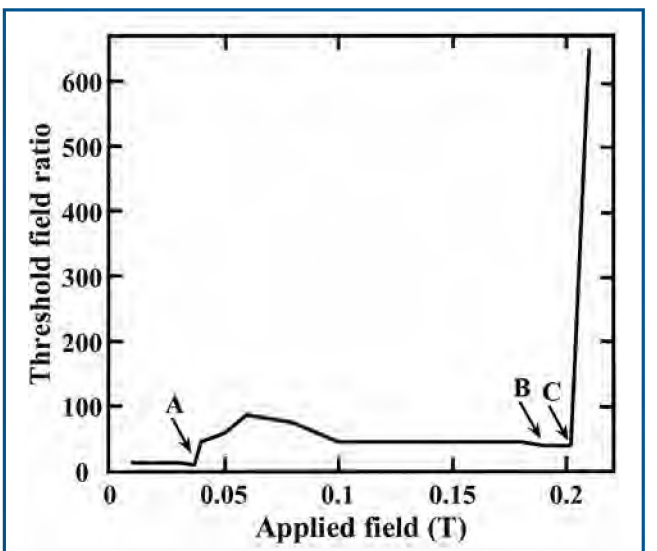

Fig. 4 Threshold field ratio (see text) plotted as a function of applied magnetic field for the same Permalloy nanowire as in Fig. 2, calculated for parallel pumping with frequency $\omega_p/2\pi = 35$ GHz. The points A, B, and C are at field values related to features on the previous dispersion curves, as explained.

distinctive features from the macroscopic case: the interaction processes involve a "mixing" between different magnon branches, and there are strong density-of-states effects for the magnons due to the spatial confinement. When the threshold strengths of the pumping field for the onset of an instabilility in any magnon branch are calculated (using techniques analogous to those for ultra-thin films [11,12]), we obtain results as in Fig. 4 for the same Permalloy nanowire considered in Fig. 2. This shows the dimensionless threshold field ratio (conventionally defined as the threshold field amplitude divided by the FMR half-linewidth in magnetic field units) plotted against the applied field for parallel pumping. Referring to the dispersion curves, the horizontal line P in Fig. 2 is drawn at half of the pumping frequency, which corresponds to production of the parametric magnons. With an applied field of 0.202 T, for which Fig. 2 is drawn, the line P coincides with the minimum in the lowest magnon branch. When the applied field is scanned up (or down) in value, the line P moves down (or up) relative to the dispersion curves. For fields above 0.202 T the line does not intersect with any magnon branch, and so the instability threshold rapidly increases. This explains the special point labeled C in Fig. 4. For lower applied field values there may in general be one or more intersection points, and so the decay is allowed. For nanostructures (as in this example) certain features on the discrete spectrum become emphasized, by contrast with the smooth behaviour (the so-called "butterfly" curve) found for macroscopic samples [2,3]. Thus we may associate points labeled B and A in Fig. 4 as corresponding to when line P coincides with the $\mathbf{k} = 0$ magnons of the lowest and next-lowest branches, respectively. Other structural features can be attributed to density-of-states effects for the quantized magnons.

CONCLUSION

It is of great interest currently to extend the work on magnon instabilities to other types of magnetic nanostructures and to their arrays (as in magnonic crystals). Also, recent experiments have reported the observation of a Bose-Einstein condensation (BEC) in a macroscopic magnon gas at room temperature [13] when driven far from equilibrium by an intense microwave pumping field. A macroscopic theoretical interpretation [14] was subsequently developed by utilizing the form of the three- and four-magnon interaction terms. Investigation of the possible occurrence of a magnon BEC in a magnetic nanostructure with spatially-confined magnons is an intriguing topic.

ACKNOWLEDGMENTS

We thank Drs. Hoa Nguyen and Arash Akbari-Sharbaf for their valuable input to current work in this field. Partial support from the Natural Sciences and Engineering Research Council of Canada is gratefully acknowledged.

REFERENCES

1. C. Kittel, *Introduction to Solid State Physics, 8th Edn.*, Wiley, 2005.
2. D.D. Stancil and A. Prabhakar, *Spin Waves: Theory and Applications*, Springer, 2009.
3. M.G. Cottam (Ed.), *Linear and Nonlinear Spin Waves in Magnetic Films and Superlattices*, World Scientific, 1994.
4. H.T. Nguyen, T.M. Nguyen, and M.G. Cottam, "Dipole-exchange Spin Waves in Ferromagnetic Stripes with Inhomogeneous Magnetization", *Phys. Rev. B*, **76**, 134413 (2007).
5. C.T. Boone, J.A. Katine, J.R. Childress, V. Tiberkevich, A. Slavin, J. Zhu, X. Cheng, and I.N. Krivorotov, "Resonant Nonlinear Damping of Quantized Spin Waves in Ferromagnetic Nanowires: A Spin Torque Ferromagnetic Resonance Study", *Phys. Rev. Lett.*, **103**, 167601 (2009).
6. H.T. Nguyen, A. Akbari-Sharbaf, and M.G. Cottam, "Spin-wave Damping in Ferromagnetic Stripes with Inhomogeneous Magnetization", *Phys. Rev. B*, **83**, 214423 (2011).
7. N. Bloembergen and S. Wang, "Relaxation Effects in Para- and Ferromagnetic Resonance", *Phys. Rev.*, **93**, 72–83 (1954).
8. H. Suhl, "The Theory of Ferromagnetic Resonance at High Signal Powers", *J. Phys. Chem. Solids*, **1**, 209–227 (1957).
9. E. Schlömann, J.J. Green, and U. Milano, "Recent Developments in Ferromagnetic Resonance at High Power Levels", *J. Appl. Phys.*, **31**, S386–S395 (1960).
10. A.G. Gurevich and G.A. Melkov, *Magnetization Oscillations and Waves*, CRC Press, 1996.
11. H.T. Nguyen and M.G. Cottam, "Theory of Spin-wave Instability Thresholds for Ultrathin Ferromagnetic Films under Parallel Pumping", *Phys. Rev. B*, **89**, 144424 (2014).
12. Z. Haghshenasfard, H.T. Nguyen, and M.G. Cottam, "Spin-wave Instability Theory for Ferromagnetic Nanostructures", *Acta Phys. Polon. A*, **127**, 192–197 (2015).
13. S.O. Demokritov, V.E. Demidov, O. Dzyapko, G.A. Melkov, A.A. Serga, B. Hillebrands, and A.N. Slavin, "Bose-Einstein Condensation of Quasi-equilibrium Magnons at Room Temperature under Pumping", *Nature*, **443**, 430–433 (2006).
14. S.M. Rezende, "Theory of Bose-Einstein Condensation in a Microwave-driven Interacting Magnon Gas", *J. Phys.: Condens. Matt.*, **22**, 164211 (2010).